

```

      CCCCCC   HHHH   HHHH   IIII   SSSSSS   AAA
CCCCCCCC   HHHH   HHHH   IIII   SSSSSSSS   AAAAA
CCCC   CCCC   HHHH   HHHH   IIII   SSSS   SSSS   AAAAAA
CCCC   CCCC   HHHH   HHHH   IIII   SSSS   SSSS   AAAA   AAAA
CCCC           HHHH   HHHH   IIII   SSSS           AAAA   AAAA
CCCC           HHHHHHHHHHH   IIII   SSSS           AAAAAAAAAA
CCCC           HHHHHHHHHHH   IIII           SSSS           AAAAAAAAAA
CCCC           HHHHHHHHHHH   IIII           SSSS           AAAAAAAAAA
CCCC   CCCC   HHHH   HHHH   IIII   SSSS   SSSS   AAAA   AAAA
CCCC   CCCC   HHHH   HHHH   IIII   SSSS   SSSS   AAAA   AAAA
CCCCCCCC   HHHH   HHHH   IIII   SSSSSSSS   AAAA   AAAA
CCCCCCC   HHHH   HHHH   IIII   SSSSSS   AAAA   AAAA

```

10th INTERNATIONAL CONGRESS OF CHEMICAL ENGINEERING, CHEMICAL EQUIPMENT  
 DESIGN AND AUTOMATION, PRAHA, CZECHOSLOVAKIA, AUGUST 26-31, 1990

Full text of the paper :

A7;126 \*I. Mazzarino, A. Barresi and G. Baldi  
 Polytech. Torino, Torino, Italy  
 Heat and mass transfer in a catalytic monolithic combustor. [1710]

Address for correspondence :

I. Mazzarino  
 Dip. Sci. Mat. Ing. Chim.  
 Politec. Torino  
 C. Duca degli Abruzzi 24  
 I-10129 Torino  
 ITALIE

# HEAT AND MASS TRANSFER IN A CATALYTIC MONOLITHIC COMBUSTOR

I.Mazzarino, A.Barresi and G.Baldi

Dip. di Scienza dei Materiali ed Ingegneria Chimica

Politecnico di Torino - Torino, Italy

## ABSTRACT

The aim of this work was to investigate the relevance of heat and mass transfer phenomena during the catalytic combustion of organic compounds at low concentrations and to evaluate the reliability and the accuracy of computer simulations of the process by simple mathematical models.

The oxidation of aromatic hydrocarbons was carried out on a monolithic Pt-cordierite catalyst with square section channels. A bench scale reactor 1" i.d. and 12.5 mm long was used. The Mars-Van Krevelen kinetic model was adopted and the kinetic constants were calculated on the basis of the experimental measured reaction rates.

A simple plug-flow model considering the heat conductivity in the solid monolith was employed to simulate the catalytic combustor. Heat and mass transfer averaged coefficients were calculated from literature correlations (Votruba et al. 1975, Hawthorn 1974). The combustor performance was expected to be affected significantly by entrance developments of the temperature and velocity profiles due to the square section and to the small length of the catalyst channels. The tabulated local Nusselt numbers by Asako and Faghri (1988) were used in order to evaluate the entrance effect. As a first approach  $Sh/Nu=1$  was adopted, but different values were also tested to show the presence of unexpected heat or mass transfer resistances.

Both steady state and transient behaviour of the reactor were tested and the temperature and concentration profiles were computed by a collocation technique. The calculated conversion vs temperature curves were plotted and compared with the experimental ones.

The experimental results show that a simple plug flow model using local heat and mass transfer coefficients and considering the heat conductivity of the solid is able to simulate with a good accuracy the behaviour of the catalytic combustor. On the contrary averaged transport coefficients do not give a satisfactory fitting between the experimental and the calculated conversions, due to the presence of entrance flow and thermal development effects.

## EXPERIMENTAL APPARATUS

A commercial Platinum catalyst supported on a cordierite honeycomb structure was used (Engelhard Torvex VOC). The main features of the catalyst are listed in table I. The catalytic monolith was placed in a thermal insulated steel reactor 1" i.d.

The schematic drawing of the experimental apparatus is shown in fig.1. The temperatures at the inlet and the outlet of the catalyst were measured by two termocouples. The flow rate of the gas phase, consisting of dust free air, was controlled by a mass flow meter. The organic component (benzene) was fed as a liquid phase by a metering pump and vaporized in a Venturi mixer by the air stream. A large size vessel was placed after the mixer to stabilize the concentration of the hydrocarbon in the reactor feed.

The temperature of the gas phase at the inlet of the reactor was controlled by an electrical preheater. Both in and out streams were sampled and analyzed by a GC to evaluate the reaction rate in the combustor.

The tested range of the operating conditions is listed in table II.

Table I - Catalyst Features

Cell Geometry	Square	Wall Thickness	0.3 mm
Cell Size	1.5 mm	Open Area	69 %
BET Area	16.3 m <sup>2</sup> /g	Diameter	22 mm
Lenght	12.4 mm		

Table II - Operating Conditions Range

Concentration	60 - 2000 ppm	Temperature	373 - 623 K
Space Velocity	20 - 75 1/s	Pressure	100 - 140 kPa

## MATHEMATICAL MODEL

A monodimensional mathematical model comprising the solid phase heat conduction was adopted to simulate the behaviour of the reacting system. The basic assumptions of this model are:

- plug flow regime of the gas phase;
- negligible gas heat conductivity;
- ideal gas behaviour;
- negligible radiant heat transport;
- adiabatic reactor.

According to these assumptions the dimensionless heat and mass balance equations in steady state conditions can be written as follows:

$$(1/Pe) \frac{d^2 \tau_s}{d\xi^2} - J_H (\tau_s - \tau_g) + B Da = 0$$

$$\frac{d\tau_g}{d\xi} - J_H (\tau_s - \tau_g) = 0$$

$$\frac{dY}{d\xi} + Da = 0$$

$$J_D \left[ \frac{(1 - Y)}{(1 + \tau_g)} - \frac{(1 - \omega)}{(1 + \tau_s)} \right] + Da = 0$$

subject to the following dimensionless form of the boundary conditions:

$$\xi = 0 \quad \tau_g = 0 \quad Y = 0 \quad \frac{d\tau_s}{d\xi} = 0$$

$$\xi = 1 \quad \frac{d\tau_s}{d\xi} = 0$$

where:

$$\tau_{s,g} = \frac{T_{s,g} - T_{go}}{T_{go}} ; \quad \xi = \frac{x}{L} ; \quad Y = \frac{Y_{go} - Y_g}{Y_{go}} ; \quad \omega = \frac{Y_{go} - Y_s}{Y_{go}}$$

$$J_H = \frac{h a_v L}{(\rho_g v)_o \eta C_p} ; \quad J_D = \frac{k a_v L}{\eta v_o} ; \quad Da = \frac{a_v L r}{v_o \eta C_o}$$

$$Pe = \frac{L (\rho_g v)_o \eta C_p}{\alpha (1-\eta)} ; \quad B = \frac{(-\Delta H) C_o}{\rho_{go} C_p T_o}$$

The adopted monodimensional model needs a preliminary definition of the heat and mass transfer coefficients. Most of the data available in the literature consist of dimensionless heat transfer coefficients (Nusselt number) calculated, under laminar flow regime and simple boundary conditions, by bi- and three-dimensional mathematical models.

In the first section of a catalytic combustor, at low temperature and conversion degree, the global rate of conversion is controlled by the kinetics of the reaction and constant wall flux can be assumed. Over the ignition point of the catalyst the system is under diffusional control, the concentration at the catalyst surface is nearly zero and constant wall temperature and concentration can be assumed.

The thermal conduction in the solid monolith is an important phenomenon because it affects the position of the ignition point of the catalyst and consequently the conversion in the reactor.

In the case of square cell monoliths the transport phenomena are strongly affected by the entrance effects. The heat and mass transfer coefficients are very high at the entrance of the channels because of the undeveloped temperature and velocity profiles, but they decrease along the reactor down to the fully developed regime values. In this case the averaged transport coefficients given by some authors (Votruba 1975, Hawthorn 1974) do not lead to a satisfactory evaluation of the combustor performance and local heat and mass transfer coefficients must be used (Asako 1988, Chandrupatla 1978, Del Giudice 1979, Shah 1979).

## EXPERIMENTAL RESULTS

The kinetic constants of the oxidation reaction were experimentally evaluated by measurements of the reaction rate in the kinetic controlled regime (low inlet temperatures). A two steps catalytic oxidation mechanism was assumed according to the Mars-van Krevelen kinetic model:

reactant + oxidated catalyst  $\rightarrow$  products + reduced catalyst

oxigen + reduced catalyst  $\rightarrow$  oxidated catalyst

The overall reaction rate is:

$$-r = \frac{k_0 k_1 C_{O_2} C}{k_0 C_{O_2} + \gamma k_1 C}$$

and  $\gamma$ , oxygen stoichiometric coefficient, is 7.5 for benzene deep oxidation.

The following values of the kinetic constants were obtained on the basis of the experimental results:

$$k_1 = 1.29 \cdot 10^{21} \exp(-20000/T) \text{ m/s}$$
$$k_o = 3.70 \cdot 10^7 \exp(-10775/T) \text{ m/s}$$

The set of differential equations of the reactor model was integrated by a collocation technique using a Fortran program running on a VAX 8800 computer. Both dynamic and steady-state conditions were tested.

When transition from kinetics controlled to diffusion controlled regime takes place along the monolith, it is difficult to obtain the convergence of the algorithm for the steady-state set of equations, due to the sharp rise of the temperature around the point where the reactor lights off. In these cases, an initial estimation of the solution, falling in the convergence range, was obtained by integration of the dynamic equations.

Figures 2 to 5 show the conversion degree as a function of the inlet gas temperature at various inlet concentrations of the hydrocarbon. In these figures the experimental data are compared with those calculated by the model using different transport coefficient correlations [Asako and Faghri(A), Votruba et al.(V) and Hawthorn(H)]. Votruba et al. give different correlations for Sh and Nu; in the other cases Sh=Nu was assumed.

The figures clearly show that the best fitting between the experimental and the calculated data is obtained in the case of local heat and mass transfer coefficients, curve(A).

Fig. 6 shows the experimental conversion degree at various gas flow rates compared with the calculated values assuming local transport coefficients.

The influence of the Nu/Sh ratio on the fitting between experimental and calculated results is shown in fig.7. The best results were obtained taking the Sherwood number from correlations and increasing the Nusselt number with respect to the calculated value. The asymptotic high temperature conversion (diffusional regime) depends mainly on the Sherwood number, but the shape of the conversion vs temperature curves is affected by the Nu/Sh ratio.

Figures 8 and 9 shows the transient behaviour of the catalytic combustor starting from the following conditions: catalyst constant temperature, zero inlet hydrocarbon concentration. A step perturbation of the inlet reactant concentration was employed to simulate the start-up of the combustor.

## CONCLUSIONS

By comparing the experimental results with the calculated conversion rates the following conclusions can be drawn:

- the behaviour of a catalytic combustor can be simulated with a satisfactory accuracy by means of a very simple model comprising the heat conduction in the solid catalyst. Heat and mass transfer coefficient referring to different boundary conditions must be employed if the transition from kinetic to diffusional control takes place along the monolith. In this case in the first part of the combustor constant wall mass and heat flux can be considered, but over the ignition point constant wall temperature and concentration must be assumed;
- most of the heat and mass transfer coefficient correlations reported in the literature are not suitable for the square cell catalyst used in this work because of the relevance of the entrance effects;
- the best results can be obtained by using local transport coefficients, due to the influence of the entrance thermal and hydrodynamic developments on the combustor behaviour.

## NOTATIONS

$a_v$	external catalyst area per unit volume, $m^2/m^3$
$C_p$	specific heat capacity of the gas phase, $kJ/(kg K)$
$C^p$	gas phase hydrocarbon concentration, $kmol/m^3$
$C_{O_2}$	gas phase oxygen concentration, $kmol/m^3$
$G_{O_2}$	volumetric flow rate at standard conditions, $l/min$
$(-\Delta H)$	reaction enthalpy, $kJ/kmol$
$h$	heat transfer coefficient, $kJ/(s m^2 K)$
$k$	mass transfer coefficient, $m/s$
$k_1$	kinetic constant, $m/s$
$k_o$	kinetic constant, $ms$
$L$	reactor length, $m$
$r$	reaction rate per unit surface, $kmol/(s m^2)$
$T$	temperature, $K$
$v$	gas phase velocity, $m/s$
$x$	axial reactor coordinate, $m$
$y$	hydrocarbon molar fraction, dimensionless
$\alpha$	thermal conductivity of the solid support, $kJ/(s m K)$
$\gamma$	oxygen stoichiometric coefficient, dimensionless
$\eta$	free cross section fractional area, dimensionless
$\rho_g$	gas phase density, $kg/m^3$

## Subscripts

$s$	catalyst surface
$o$	inlet conditions
$g$	gas phase

## REFERENCES

R.D.Hawthorn, AIChE Symp. Ser. **70**, n.137, 428 (1974)

J.Votruba, J.Sinkule, V.Hlavaček and J.Skrivanek, Chem. Eng. Sci. **30**, 117 (1975)

A.R.Chandrupatla and V.M.K.Sastri, Numerical Heat Transfer **1**, 243 (1978)

R.K.Shah and A.L.London, Laminar Flow Forced Convection in Ducts, (1978)

S.Del Giudice, M.Strada and G.Comini, Num. Heat Transfer **2**, 487 (1979)

Y.Asako and M.Faghri, Journal of Heat Transf. **110**, 855 (1988)

## Aknowledgments

The authors are in debt to Dr M. Vanni for valuable discussions and to A. Mussinatto for computational work. Financial support was given by Italian National Research Council (C.N.R.). The catalyst was kindly supplied by Engelhard Corp.

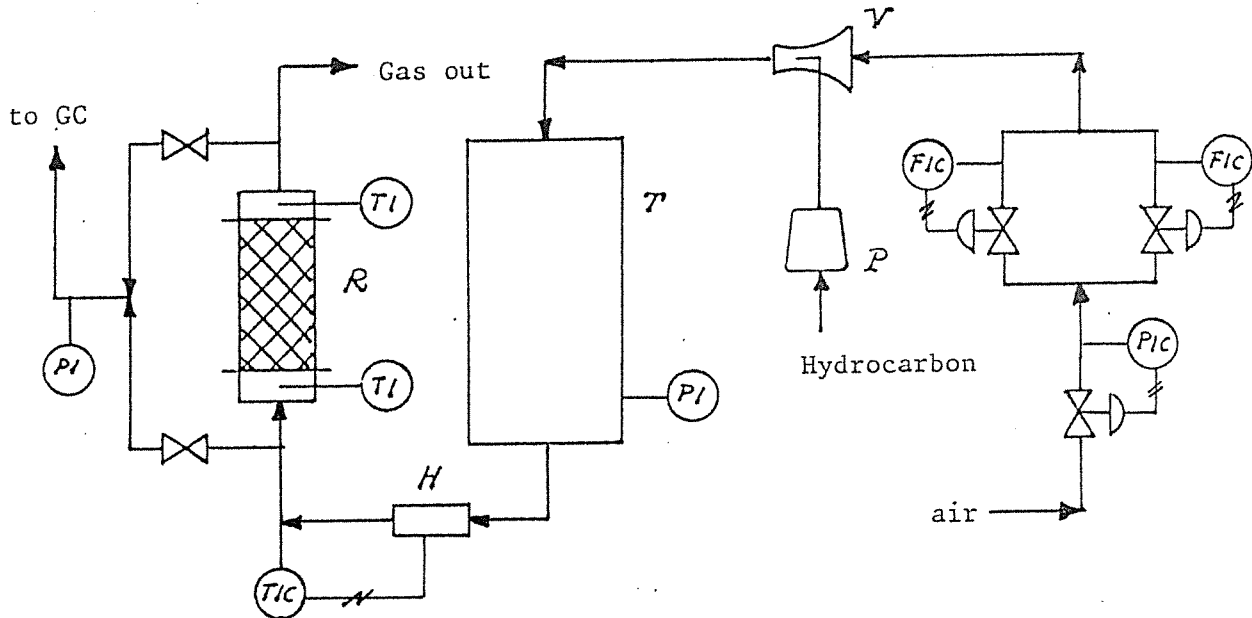


Fig.1 - Experimental Apparatus: R catalytic combustor, P metering pump, V venturi mixer, T buffer vessel, H heater

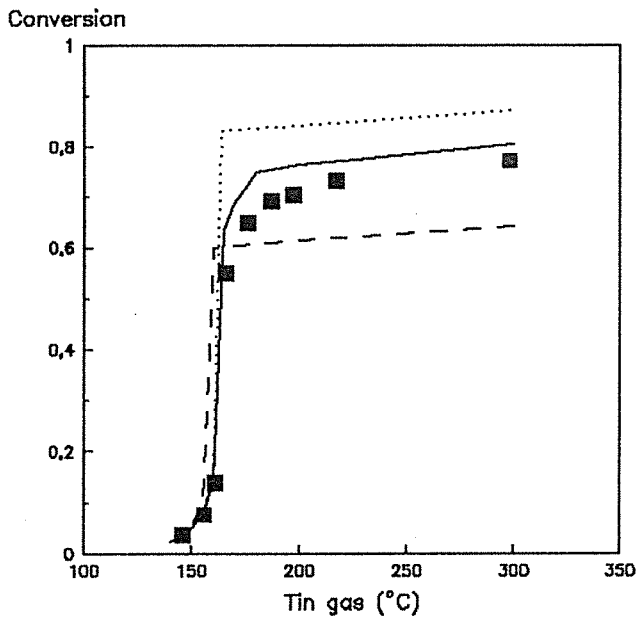


Fig.2 - Conversion vs temperature,  $C_0=1000$  ppm  
 $G=10.6$  l/min. ■ experimental data, calculated:  
 — (A), - - (V), .....(H)

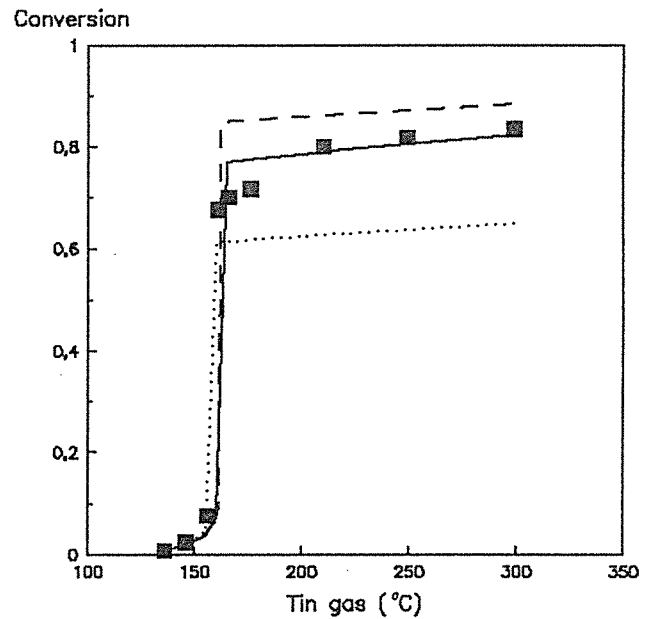


Fig.3 - Conversion vs temperature,  $C_0=2000$  ppm  
 $G=10.6$  l/min. ■ experimental data, calculated:  
 — (A), .....(V), - - - (H)

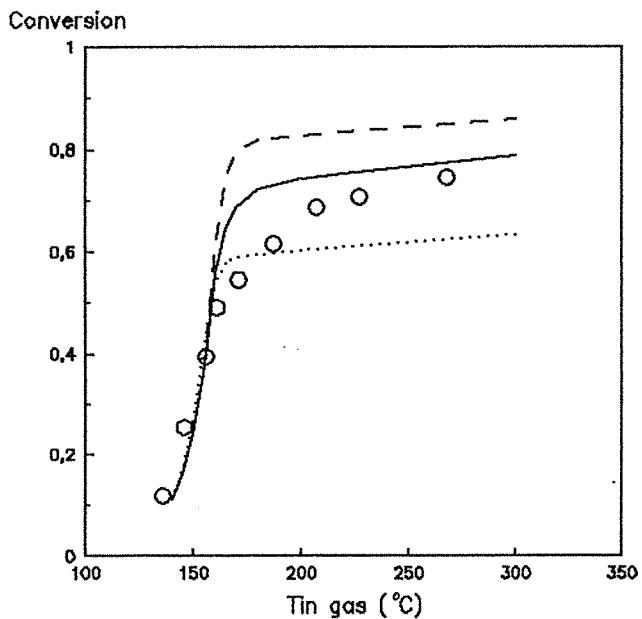


Fig.4 - Conversion vs temperature,  $C_0=200$  ppm  
 $G=10.6$  l/min. ○ experimental data, calculated:  
 — (A), .....(V), - - - (H)

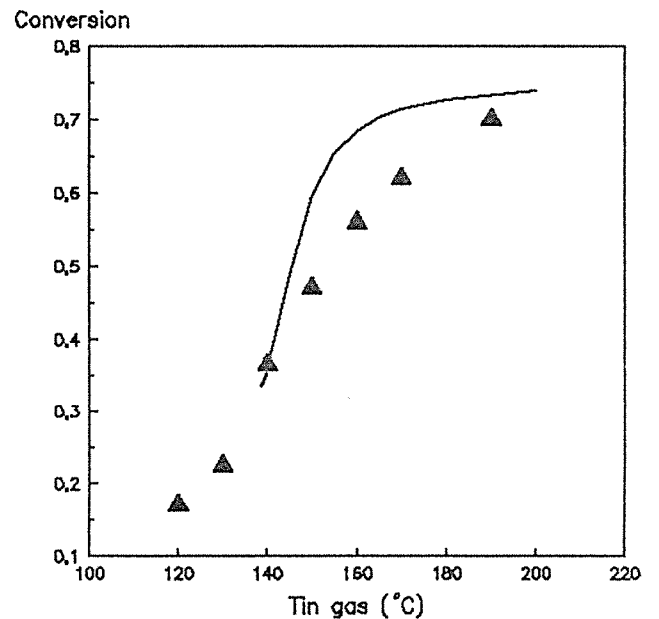


Fig.5 - conversion vs temperature,  $C_0=60$  ppm  
 $G=10.6$  l/min. ▲ experimental data, — calc. (A)

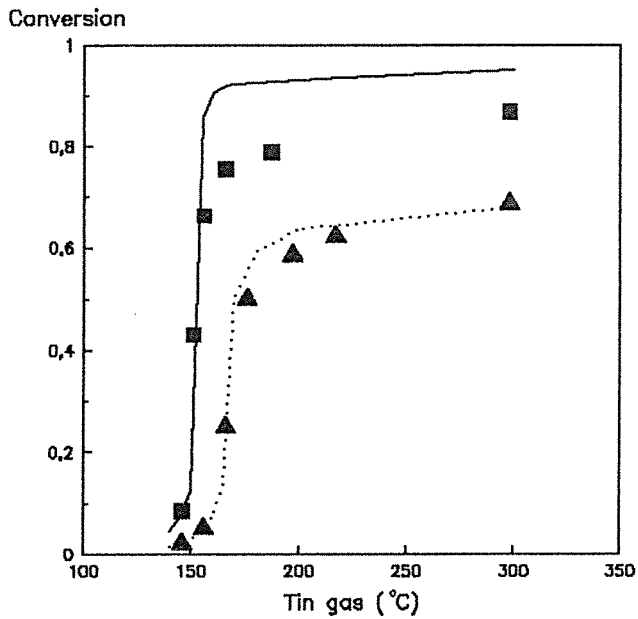


Fig.6 - Conversion vs temperature,  $C_o=1000$  ppm  
 $G=5.6$  l/min: ■ experimental, — calculated (A)  
 $G=15.6$  l/min: ▲ experimental, .....calculated (A)

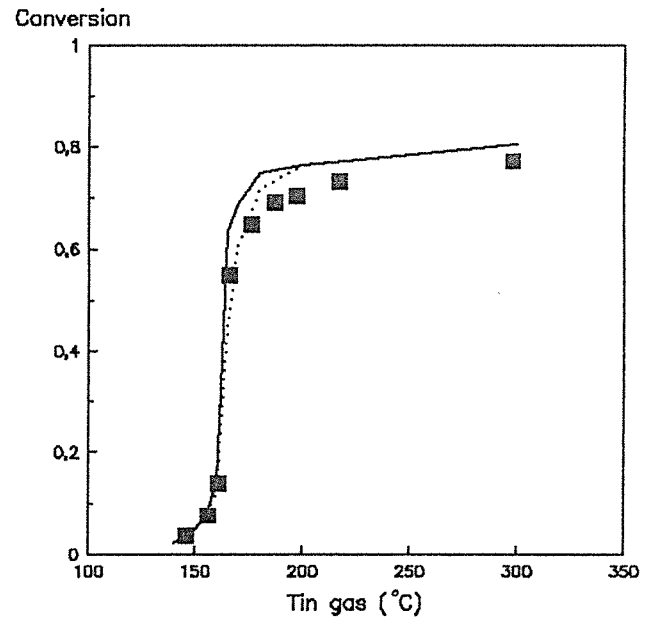


Fig.7 - Conversion vs temperature,  $C_o=1000$  ppm  
 $G=10.6$  l/min. ■ experimental data, calculated:  
 — Sh from (A)  $Nu=Sh$ , .....Sh from (A)  $Nu=2Sh$

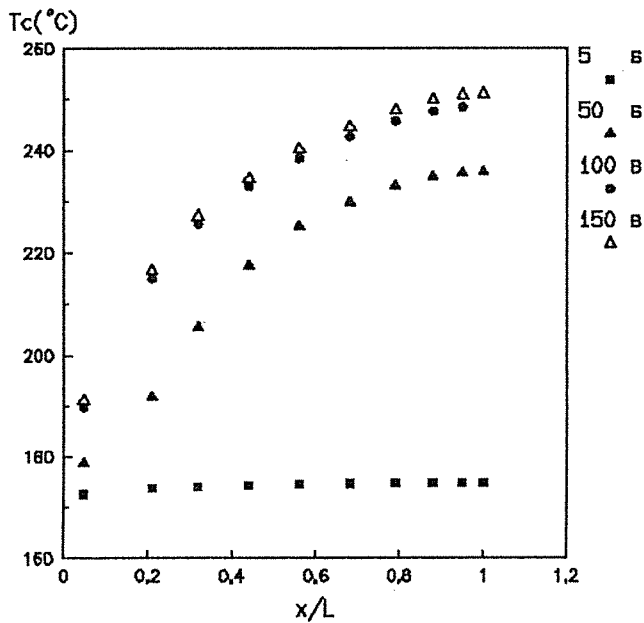


Fig.8 - Calculated (A) catalyst temperature vs reactor length in dynamic regime,  $C_o=1000$  ppm  
 $G=10.6$  l/min and Tin gas=170°C.

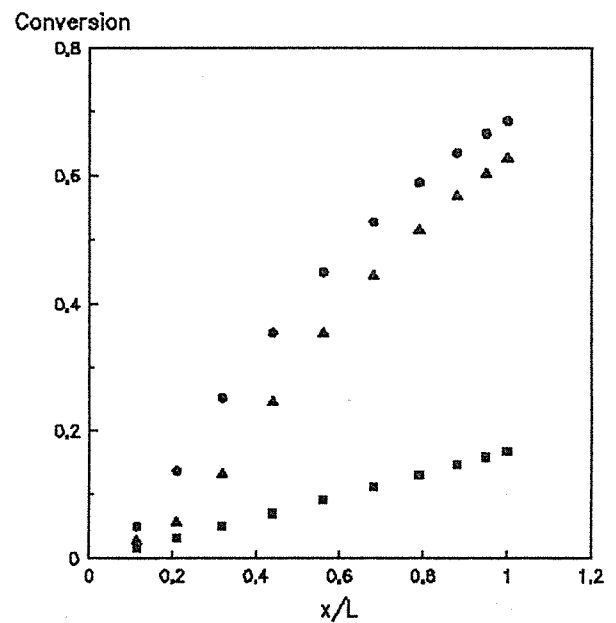


Fig.9 - calculated (A) gas phase conversion vs reactor length in dynamic regime,  $C_o=1000$  ppm  
 $G=10.6$  l/min and Tin gas=170°C.